Coordinated Control of quadcopters for large object positioning

Maria Inês Ribeiro Soares
maria.soares@tecnico.ulisboa.pt

Instituto Superior Técnico, Lisboa, Portugal

September 2021

Abstract

In recent years, unmanned aerial vehicles such as drones have been gaining prominence as alternatives for performing several tasks. Although this type of vehicle has undergone several improvements in a short period of time, in most cases its flight time is not yet long enough to allow certain missions to run only with the autonomy of a single vehicle. Additionally, the transport of large objects in general is not feasible with a single drone. It is therefore necessary to consider the intervention of two or more vehicles. In this context, this study aims to develop a controller for a multi-drone system, in order to allow the transportation of objects that cannot be handled by just one vehicle. To this end, different models were analyzed in order to characterize several scenarios of object transport, including a 2D scenario with two birotors transporting a load and a 3D scenario with two quadrotors transporting a load restricted to keep a horizontal configuration. Furthermore, the question of drone autonomy and the replacement of vehicles was addressed, considering a mission scenario that goes beyond the capabilities of the energy stored in a single vehicle and requires drone replacement to be performed. The problem addressed involved optimizing the time instants for executing the take-off of a replacement drone and determining the meeting point between the two drones, taking energy consumption into account. The control strategy used for the development of this controller is based on non-linear model predictive control (NMPC) algorithms. Backed with simulation results, it is shown that the cooperation of vehicles for the purpose of carrying out the transport task is feasible, under certain assumptions. Additionally, the vehicle replacement problem is implemented and tested, based on an energy consumption model defined for each vehicle involved in the transport task. The numerical simulations were created in MATLAB resorting to the solvers fmincon and ode45 and its results verify the effectiveness of the proposed control strategies for both problems.
Keywords: Drones, Model Predictive control, multi-drone system, replacement of vehicles.

1. Introduction

1.1. Motivation

Although initially conceived for military purposes, drones have nowadays a wide spectrum of applications which has resulted in their rapid development and adaptation to various scenarios and environments to carry out challenging missions. There are many fields where the presence of these vehicles can bring added-value. One such example is agriculture. This sector has been increasingly challenged due to climate change. In fact, according to FAO[1] and ITU[2], the world population and food production worldwide will have to increase by 70% by 2050 [4]. Drones can greatly reduce the costs of this action through analysis of soils and fields, crop monitoring, aerial planting, irrigation, among others [3]. Another area where drones can make a difference is multimedia and film applications. Most films have motion sequences whose image needs to be obtained from different angles, which requires installing multiple cameras in different places or adopting a better alternative: using drones. The performance of these vehicles has increased more and more in this area. However, there are still several challenges such as estimating the actor's position, understanding the context of the scene at an artistic level and operating in scenarios without prior information [5]. The versatility of drones in various contexts has increased interest of researchers in exploring the cooperation of these vehicles in order to solve increasingly complex problems. One of these problems is the transport of large objects. In this context, the present study addresses the situation in which a single vehicle cannot handle a large object and, therefore, the need for cooperation between two or more of these vehicles arises. In this scenario, the problem of drone autonomy will also be addressed so that the mission to be carried out is not interrupted.

[1] Food and Agriculture Organization of the United Nations.

[2] International Telecommunication Union

1.2. State of the Art

Since the late 1980s, model predictive control (MPC) has gained prominence as an optimization technique due to its distinct ability to incorporate constraints. In particular, the appearance of nonlinear predictive control allowed the development of controllers that deal with nonlinearities present in the dynamics of the models, which further extended the scope of MPC applications. In fact, this control strategy can be very efficient in controlling systems such as UAVs as seen in [7], where the authors control a quadcopter using this technique, taking into account restrictions to the problem. Recently, the assignment of cooperative tasks for multi-drone systems has been extensively studied, with different models and algorithms already proposed. One such example is [8], that presents a multi-drone approach to autonomous cinematography planning where an architecture based on a cooperative team is proposed. This new application raises a series of challenges since vehicles are expected to make decisions in real time and to capture images autonomously, while following guidelines present in typical filming of cinematography rules. This thesis explores another application of multi-drone systems: the transport of objects large enough that require two or more vehicles to perform the task. This situation was addressed in [9], where the authors present a configuration where a set of drones are rigidly connected to the object to be transported. In the present study, a different approach is adopted that considers a configuration where each drone is connected to the object by an articulation, which allows the total mobility of the vehicle, that moves with the usual four degrees of freedom. Additionally, a centralized control approach is considered, in contrast to the one presented in [9], which is implemented through a decentralized controller. It is also important to address the problem of drone autonomy, especially in missions that depend on more than one vehicle, since its battery is a limited resource. There are several solutions for extending a UAV mission. The approach considered in this work is based on the replacement of vehicles in order to ensure the continuity of the assigned task. A relevant article that addresses this issue is [6], applied to the area of structural inspection. For this purpose, the authors propose a continuity-of-service algorithm based on an extension of the MAVLink protocol that implements the replacement of vehicles automatically, through messages and commands that allow communication between drones.

2. Extended Abstract Outline

The extended abstract is organized as follows

section 3 presents the problem formulation, where the configuration of the system, its limitations and assumptions are addressed. In **section 4**, four different systems are modeled, where their limitations and assumptions are explained, based on the study of the bi-rotor and the quadcopter. **section 5** presents the problem of control of the system composed of two bi-rotors and a bar. **section 6** addresses the development of the control strategy for the transportation of a bar through the cooperation of two drones. In **section 7** , the drone autonomy problem is also analyzed and solved through a vehicle replacement strategy. In **section 8**, the simulation results for each of the problems addressed are presented. Finally, in **section 9**, the findings of this study are discussed and recommendations are made for future improvements in the results obtained.

3. Problem formulation

The central problem of this dissertation is the transportation of large objects by a multi-drone system. This system is composed of two quadcopters and a bar. The drones and the bar are connected through spherical joints that allow both vehicles to move with freedom of movement, without compromising the transport of this object. Fig. 1 shows this configuration, where the joints are represented by two circles, connecting each vehicle to the object.

Figure 1: Configuration of the quadcopter bar system.

For this problem, the following premises are assumed

1. The movement of the system in two dimensions (x and y) is decoupled from the longitudinal movement. In other words, these two separate movements are considered since the system moves at $z = 0$, where the three rotation angles of drone i (ϕ_i, θ_i, ψ_i, $i = 1, 2.$) are considered as the angle of the bar around the z axis, ψ_b.

2. The bar has a defined length c and negligible width and height.

3. The center of mass of the system coincides with the center of mass of the bar.

4. Both vehicles have autonomy to carry out the task of transport until the end.

Throughout the work, an analysis of four different models is carried out, with increasing complexity, where the last situation addressed corresponds to the quadcopter bar system described in this section.

4. Systems modeling

4.1. Bi-rotor model

Consider the planar model of a drone, with mass m and two rotors, represented in Fig. 2. The bi-rotor moves with an angle θ in relation to the horizontal plane, known as its pitch angle. Additionally, b corresponds to the distance between each rotor and the center of mass of the UAV, F_g corresponds to the force of gravity, f_1 and f_2 correspond to the forces generated by each rotor of the vehicle, and $f = f_1 + f_2$ corresponds to the total thrust exerted by the vehicle rotors.

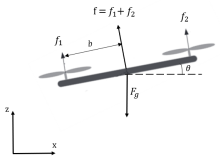

Figure 2: Bi-rotor model, adapted from [2].

In order to define the dynamics of the bi-rotor, the Euler-Lagrange equation is considered. The generalized coordinates of this system fully describe it and are given by

$$q = \begin{bmatrix} x & z & \theta \end{bmatrix}^T, \tag{1}$$

where x and z correspond to the position of the vehicle and θ to its pitch angle. The kinetic energy (K) and the potential energy (U) of the system are given by

$$\begin{aligned} K(q,\dot{q}) &= \frac{1}{2}m\dot{x}^2 + \frac{1}{2}m\dot{z}^2 + \frac{1}{2}I\dot{\theta}^2, \\ U(q) &= mgz, \end{aligned} \tag{2}$$

where I corresponds to the UAV moment of inertia. Considering the Lagrangian function $L = K(q,\dot{q}) - U(q)$, the Euler-Lagrange equation takes the form

$$\frac{\partial}{\partial t}\left(\frac{\partial L}{\partial \dot{q}}\right) - \frac{\partial L}{\partial q} = \begin{bmatrix} -f\sin(\theta) & f\cos(\theta) & \tau \end{bmatrix}^T. \tag{3}$$

Finally, the dynamics of the vehicle can be written as

$$\begin{aligned} I\ddot{\theta} &= b(f_1 - f_2), \\ m\begin{bmatrix} \ddot{x} \\ \ddot{z} \end{bmatrix} &= \begin{bmatrix} 0 \\ -mg \end{bmatrix} + R(\theta)\begin{bmatrix} 0 \\ f_1 + f_2. \end{bmatrix}, \end{aligned} \tag{4}$$

where $R(\theta)$ is the following rotation matrix

$$R(\theta) = \begin{bmatrix} cos(\theta) & -sin(\theta) \\ sin(\theta) & cos(\theta) \end{bmatrix}. \tag{5}$$

4.2. Bi-rotor bar model

Consider two bi-rotors, with masses m_1 and m_2, that cooperate in order to carry a bar of length c, negligible width and mass m_b that is articulated to both vehicles. The configuration of this articulation allows both vehicles to move with freedom of movement. Fig. 3 shows the bi-rotor bar system, where the position of each rigid body is defined in the inertial frame, $\{I\}$, as follows

$$p^I_{D_1} = \begin{bmatrix} x_1 \\ z_1 \end{bmatrix}, \quad p^I_{D_2} = \begin{bmatrix} x_2 \\ z_2 \end{bmatrix}, \quad p^I_{bar} = \begin{bmatrix} x_b \\ z_b \end{bmatrix}. \tag{6}$$

It is also possible to observe the pitch angles of each bi-rotor, θ_1 and θ_2. Each time the bar is not parallel to the horizontal plane, it assumes a rotation angle, called θ_b. Furthermore, the forces generated by each rotor (F_1, F_2, F_3, F_4) and the total thrust force exerted on each vehicle are represented, which are defined for each bi-rotor as follows

$$T_1 = F_1 + F_2, \quad T_2 = F_3 + F_4. \tag{7}$$

The pitch moments derived by the rotors of each UAV are given by

$$\tau_1 = b(F_1 - F_2), \quad \tau_2 = b(F_3 - F_4). \tag{8}$$

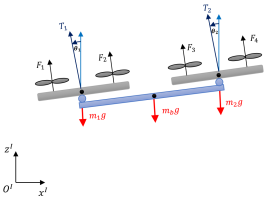

Figure 3: Bi-rotor model.

The definition of the dynamics of this system is the result of the solution of the Euler-Lagrange equation, satisfied by the generalized coordinates of the system. In this example, it is assumed that the center of mass of the system coincides with the center of mass of the bar. Thus, this system is described in its entirety through the following generalized coordinates

$$q = \begin{bmatrix} x_b & z_b & \theta_1 & \theta_2 & \theta_b \end{bmatrix}^T, \tag{9}$$

that are composed by the position of the bar (x_b and z_b), the pitch angles of each vehicle (θ_1 and θ_2) and the rotation angle of the bar, θ_b, performed in the xz-plane. The kinetic energy (K) and the potential energy (U) of the system are given by

$$\begin{aligned} K(q,\dot{q}) &= \frac{1}{2}m_b\dot{x}_b^2 + \frac{1}{2}m_b\dot{z}_b^2 + \frac{1}{2}m_1\dot{x}_1^2 + \frac{1}{2}m_1\dot{z}_1^2 + \\ &+ \frac{1}{2}m_2\dot{x}_2^2 + \frac{1}{2}m_2\dot{z}_2^2 + \frac{1}{2}I_b\dot{\theta}_b^2 + \frac{1}{2}I_1\dot{\theta}_1^2 + \frac{1}{2}I_2\dot{\theta}_2^2, \\ U(q) &= m_b g z_b + m_1 g z_1 + m_2 g z_2, \end{aligned} \tag{10}$$

where I_b corresponds to the moment of inertia of the bar and I_1 and I_2 correspond to the moments of inertia of each vehicle. Since both vehicles have the same mass, the following simplification is adopted: $m_1 = m_2 = m$.

It is remarked that the positions of both bi-rotors, $p^I_{D_1}$ and $p^I_{D_2}$, can be defined through the bar generalized coordinates, x_b, z_b and θ_b, and are given by

$$\begin{aligned} x_1 &= x_b - \frac{c}{2}\cos(\theta_b), \quad x_2 = x_b + \frac{c}{2}\cos(\theta_b), \\ z_1 &= z_b - \frac{c}{2}\sin(\theta_b), \quad z_2 = z_b + \frac{c}{2}\sin(\theta_b). \end{aligned} \tag{11}$$

Moreover, their respective derivatives are

$$\begin{aligned} \dot{x}_1 &= \dot{x}_b + \frac{c}{2}\dot{\theta}_b \sin(\theta_b), \quad \dot{x}_2 = \dot{x}_b - \frac{c}{2}\dot{\theta}_b \sin(\theta_b), \\ \dot{z}_1 &= \dot{z}_b - \frac{c}{2}\dot{\theta}_b \cos(\theta_b), \quad \dot{z}_2 = \dot{z}_b + \frac{c}{2}\dot{\theta}_b \cos(\theta_b). \end{aligned} \tag{12}$$

The Lagrangian function, $L = K(q, \dot{q}) - U(q)$, must be written taking into account the generalized coordinates defined in (9). For this purpose, the linear velocities of both vehicles ($\dot{x}_1$, $\dot{z}_1$, $\dot{x}_2$ and $\dot{z}_2$) are replaced by its equivalent expressions defined in (12). Hence, the following Lagrangian function is obtained

$$\begin{aligned} L = &(\frac{1}{2}m_b + m)\dot{x}_b^2 + (\frac{1}{2}m_b + m)\dot{z}_b^2 + m\frac{c^2}{4}\dot{\theta}_b + \\ &+ \frac{1}{2}I_b\dot{\theta_b}^2 + \frac{1}{2}I_1\dot{\theta_1}^2 + \frac{1}{2}I_2\dot{\theta_2}^2 - (m_b + 2m)gz_b. \end{aligned} \tag{13}$$

The dynamics of the bi-rotor are defined through the Euler-Lagrange equation, which are given by

$$\tfrac{\partial}{\partial t}(\tfrac{\partial L}{\partial \dot{q}}) - \tfrac{\partial L}{\partial q} = F, \tag{14}$$

where F are the generalized forces that act on the system. In order to define vector F, it is required to decompose the forces present in this system. Fig. 4 shows the decomposition of the total thrust force exerted on each bi-rotor, T_1 and T_2, in the x and z directions, that are given by

$$\begin{aligned} T_{1_x} &= -T_1 \sin(\theta_1), \quad T_{1_z} = T_1 \cos(\theta_1), \\ T_{2_x} &= -T_2 \sin(\theta_2), \quad T_{2_z} = T_2 \cos(\theta_2). \end{aligned} \tag{15}$$

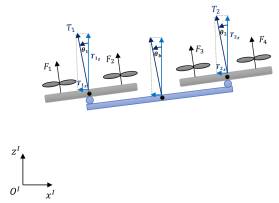

Figure 4: Decomposition of the total thrust force of both vehicles and the total force exerted on the bar.

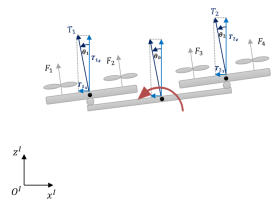

Figure 5: Decomposition of the total force exerted on the bar by both vehicles.

In Fig. 5, the positive direction of rotation of the system is represented in red, which corresponds to a counterclockwise rotation. Taking into account the direction of this rotation, T_b is calculated as follows

$$T_b = T_2 \cos(\theta_2 - \theta_b) - T_1 \cos(\theta_1 - \theta_b). \tag{16}$$

Finally, the Euler-Lagrange equation is given by

$$\tfrac{\partial}{\partial t}(\tfrac{\partial L}{\partial \dot{q}}) - \tfrac{\partial L}{\partial q} = \begin{bmatrix} -T_1 \sin(\theta_1) - T_2 \sin(\theta_2) \\ T_1 \cos(\theta_1) + T_2 \cos(\theta_2) \\ \tau_1 \\ \tau_2 \\ T_2 \cos(\theta_2 - \theta_b) - T_1 \cos(\theta_1 - \theta_b) \end{bmatrix}. \tag{17}$$

System dynamics

The equations of motion of the system derived from (17) are given by

$$\begin{aligned} &\ddot{\theta}_1 = \tfrac{\tau_1}{I_1}, \\ &\ddot{\theta}_2 = \tfrac{\tau_2}{I_2}, \\ &\ddot{\theta}_b = \tfrac{T_2 \cos(\theta_2 - \theta_b) - T_1 \cos(\theta_1 - \theta_b)}{I_b + m\frac{c^2}{2}}, \\ &(2m + m_b)\begin{bmatrix} \ddot{x}_b \\ \ddot{z}_b \end{bmatrix} = \begin{bmatrix} 0 \\ (-2m + m_b)g \end{bmatrix} + R(\theta_1)\begin{bmatrix} 0 \\ T_1 \end{bmatrix} + R(\theta_2)\begin{bmatrix} 0 \\ T_2 \end{bmatrix}. \end{aligned} \tag{18}$$

4.3. Quadcopter model

A quadcopter is a three-dimensional drone with four rotors. The model of the quadcopter is defined as a rigid body with four degrees of freedom (DOF) in free flight: three DOF with respect to attitude and one DOF with respect to the total thrust force applied to the vehicle. The position and orientation of a quadcopter are described through two coordinate frames: an inertial frame, $\{I\}$, which is fixed to the Earth, and a body frame, $\{B\}$, which is fixed to the center of mass of the UAV, both represented in Fig. 6. In $\{I\}$, the unit vectors $\{e_1, e_2, e_3\}$ match the x, y and z axes, respectively. The position and velocity of the quadcopter is denoted in the inertial frame by

$$p^I = p = \begin{bmatrix} x & y & z \end{bmatrix}^T, \quad \dot{p} = \begin{bmatrix} \dot{x} & \dot{y} & \dot{z} \end{bmatrix}^T.$$

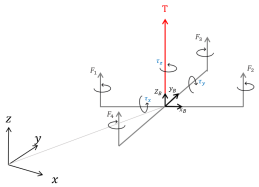

Figure 6: Coordinate systems and the forces and moments generated by the quadrotor rotors.

The rotation angles used to represent the orientation of this vehicle are the $Z-Y-X$ Euler angles, and are given by $\Theta = \begin{bmatrix} \phi & \theta & \psi \end{bmatrix}^T$, which correspond to roll, pitch and yaw rotations, respectively [11]. The transformation from the body frame to the inertial frame is given by three consecutive rotations around the three defined axes, using the $Z-Y-X$ Euler angles convention. The rotation matrix between the body frame and the inertial frame is defined, through the referred rotations.

$$\begin{aligned} R_B^I &= R_z(\psi)R_y(\theta)R_x(\phi) = R_z(\psi_b - \psi)R_y(\theta)R_x(\phi) \\ &= \begin{bmatrix} \cos\psi\cos\theta & \cos\psi\sin\theta\sin\phi - \sin\psi\cos\phi & \cos\psi\sin\theta\cos\phi + \sin\psi\sin\phi \\ \sin\psi\cos\theta & \sin\psi\sin\theta\sin\phi + \cos\psi\cos\phi & \sin\psi\sin\theta\cos\phi - \cos\psi\sin\phi \\ -\sin\theta & \cos\theta\sin\phi & \cos\theta\cos\phi \end{bmatrix}. \end{aligned} \tag{19}$$

Note that the linear velocities of this vehicle, given by $\dot{p} = \begin{bmatrix} \dot{x} & \dot{y} & \dot{z} \end{bmatrix}^T$, can be transformed, in order to be expressed in the body reference, as follows $v^B = \begin{bmatrix} v_x & v_y & v_z \end{bmatrix}^T$. Similarly, the angular velocities of the quadcopter expressed in $\{I\}$, given by $\dot{\Theta} = \begin{bmatrix} \dot{\phi} & \dot{\theta} & \dot{\psi} \end{bmatrix}^T$, can be transformed into angular velocities expressed in $\{B\}$, $w^B = \begin{bmatrix} w_x & w_y & w_z \end{bmatrix}^T$.

Actuation

Fig. 6 shows the four forces (F_1, F_2, F_3 and F_4) that are generated by the quadcopter rotors. Through these forces, the total force exerted on the vehicle, T, and the rolling, τ_x, pitching, τ_y and yawning, τ_z moments, can be defined as follows

$$\begin{aligned} T &= \sum_{i=1}^{4} F_i = F_1 + F_2 + F_3 + F_4, \\ \tau^B &= \begin{bmatrix} \tau_x \\ \tau_y \\ \tau_z \end{bmatrix} = \begin{bmatrix} d(F_2 - F_3) \\ d(F_1 - F_3) \\ c(F_1 + F_3 - F_2 - F_4) \end{bmatrix}, \end{aligned} \tag{20}$$

where d is the distance between each rotor and center of mass of the vehicle and c is a constant coefficient for the induced torque of the motor [10].

Quadcopter dynamics

The rotational dynamics of the quadcopter, expressed in $\{B\}$, is given by

$$I\dot{w}^B = -w^B \times Iw^B + \tau^B, \tag{21}$$

where the inertial matrix, I, is defined as follows

$$I = \begin{bmatrix} I_{xx} & 0 & 0 \\ 0 & I_{yy} & 0 \\ 0 & 0 & I_{zz} \end{bmatrix}.$$

The translational dynamics of the quadcopter are expressed in $\{I\}$, and are given by

$$m\ddot{p} = -mge_3 + TR_B^I e_3, \tag{22}$$

where m is the mass of the quadcopter and g is the force of gravity. Together, Equations (21) and (22) completely characterize the movement of this vehicle.

4.4. Quadcopters transporting a bar

Consider a situation in which two quadcopters, with masses m_1 and m_2, carry a bar of length l and of negligible width and height, through spherical joints that allow both vehicles to rotate. The coordinate frames defined for this problem are the inertial frame, $\{I\}$, the body frame, $\{B_i\}$, of each of the drones ($i = 1, 2$), and the body frame of the bar, $\{O\}$. The positions of the three rigid bodies are given in the inertial frame, respectively, by

$$p_{D_1} = \begin{bmatrix} x_1 \\ y_1 \\ z_1 \end{bmatrix}, \quad p_{D_2} = \begin{bmatrix} x_2 \\ y_2 \\ z_2 \end{bmatrix}, \quad p_{bar} = \begin{bmatrix} x_b \\ y_b \\ z_b \end{bmatrix}. \tag{23}$$

In this problem, the system moves strictly at $z = 0$ and only its movement in the xy-plane is analyzed. Thus, the rotation angles considered for each body are $\Theta_1 = \begin{bmatrix} \phi_1 & \theta_1 & \psi_1 \end{bmatrix}^T$, $\Theta_2 = \begin{bmatrix} \phi_2 & \theta_2 & \psi_2 \end{bmatrix}^T$, and ψ_b. Fig. 7 shows the Z rotation of the three rigid bodies.

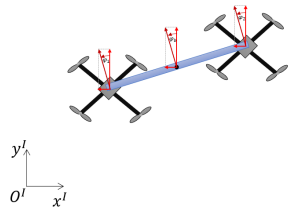

Figure 7: System of two quadcopters carrying a bar - top view.

In order to define the dynamics of the system, the rotation matrix, R_{Bi}^O, which describes the rotation between $\{B_i\}$ and $\{O\}$, must be described. For this purpose, it is required to first define the rotation matrix, R_O^I, which defines the rotation between the body frame of the bar and the inertial frame. Hence, R_O^I is defined considering the Z rotation of the Euler angles, and its definition is given by

$$R_O^I = \begin{bmatrix} \cos\psi_b & -\sin\psi_b & 0 \\ \sin\psi_b & \cos\psi_b & 0 \\ 0 & 0 & 1 \end{bmatrix}. \tag{24}$$

R_{Bi}^O can now be defined. For the sake of simplicity of calculations, a generic body frame, $\{B\}$, is considered.

$$\begin{aligned} &R_B^O = R_I^O R_B^I = (R_O^I)^T R_B^I = R_z(\psi - \psi_b) R_y(\theta) R_x(\phi) = \\ &= \begin{bmatrix} \cos(\psi_b - \psi)\cos\theta & \sin(\psi_b - \psi)\cos\phi + \cos(\psi_b - \psi)\sin\theta\sin\phi & -\sin(\psi_b - \psi)\sin\phi + \cos(\psi_b - \psi)\sin\theta\cos\phi \\ \sin(\psi - \psi_b)\cos\phi & \cos(\psi_b - \psi)\cos\phi + \sin(\psi - \psi_b)\sin\theta\sin\phi & -\cos(\psi_b - \psi)\sin\phi + \sin(\psi - \psi_b)\sin\theta\cos\phi \\ -\sin\theta & \cos\theta\sin\phi & \cos\theta\cos\phi \end{bmatrix}. \end{aligned} \tag{25}$$

Translational dynamics of the system

In this problem, it is assumed that the center of mass of this system coincides with the center of mass of the bar. Thus, the translational dynamics of the system is given by

$$m_{sys}\ddot{p}_b^I = -m_{sys}ge_3 + T_O, \tag{26}$$

where $m_{sys} = m_1 + m_2 + m_b$ corresponds to the total mass of the system and T_O is the total force applied by the vehicles on the bar, given by

$$\begin{aligned} T_O &= R_{B1}^I \begin{bmatrix} 0 \\ 0 \\ T_1 \end{bmatrix} + R_{B2}^I \begin{bmatrix} 0 \\ 0 \\ T_2 \end{bmatrix} = \\ &= \begin{bmatrix} (\cos\psi_1 \sin\theta_1 \cos\phi_1 + \sin\psi_1 \sin\phi_1)T_1 \\ (\sin\psi_1 \sin\theta_1 \cos\phi_1 - \cos\psi_1 \sin\phi_1)T_1 \\ \cos\theta_1 \cos\phi_1 T_1 \end{bmatrix} + \\ &+ \begin{bmatrix} (\cos\psi_2 \sin\theta_2 \cos\phi_2 + \sin\psi_2 \sin\phi_2)T_2 \\ (\sin\psi_2 \sin\theta_2 \cos\phi_2 - \cos\psi_2 \sin\phi_2)T_2 \\ \cos\theta_2 \cos\phi_2 T_2 \end{bmatrix}. \end{aligned} \tag{27}$$

Rotational dynamics of the system

Each rigid body has its own rotational dynamics, given by

$$\begin{aligned} I\dot{w}^{B_1} &= -w^{B_1} \times Iw^{B_1} + \tau^{B_1}, \\ I\dot{w}^{B_2} &= -w^{B_2} \times Iw^{B_2} + \tau^{B_2}, \\ I_{sys}\dot{w}^O &= -w^O \times I_{sys}w^O + \tau^O, \end{aligned} \tag{28}$$

where I_{sys} is the moment of inertia of the system, I corresponds to the moments of inertia of both UAV, τ^{B_1} and τ^{B_2} correspond to the torque exerted on each vehicle and τ^O is the total torque applied by the vehicles on the bar, defined as follows

$$\tau^O = \begin{bmatrix} L \\ 0 \\ 0 \end{bmatrix} \times R^O_{B1} \begin{bmatrix} 0 \\ 0 \\ T_1 \end{bmatrix} - \begin{bmatrix} L \\ 0 \\ 0 \end{bmatrix} \times R^O_{B2} \begin{bmatrix} 0 \\ 0 \\ T_2 \end{bmatrix} = \begin{bmatrix} 0 \\ -L\cos\theta_1\cos\phi_1 T_1 + L\cos\theta_2\cos\phi_2 T_2 \\ (-\cos(\psi_b-\psi_1)\sin\phi_1 + \sin(\psi_1-\psi_b)\sin\theta_1\cos\phi_1)T_1 L + (\cos(\psi_b-\psi_2)\sin\phi_2 + \sin(\psi_2-\psi_b)\sin\theta_2\cos\phi)T_2 L \end{bmatrix}. \tag{29}$$

5. Control of the bi-rotors bar system

In this section, the control strategy applied to the bi-rotor bar system is presented. The dynamics of this system is shown in eq.(18) present in section 4.2.

Cost function

In this example, the control objectives are system stabilization and trajectory optimization. Therefore, the quadratic function is a suitable choice because its minimization leads to an optimal global solution. The cost function is given by

$$\begin{aligned} J = \sum_{i=1}^{H} &[(X(k+i) - X^*(k+i))^T Q (X(k+i) - X^*(k+i)) + \\ &+ (U(k+i) - U^*(k+i))^T R_Q (U(k+i) - U^*(k+i))] \end{aligned} \tag{30}$$

where Q and R_Q correspond, respectively, to the weight factors that are applied to the states and to the control inputs.

Optimization problem

Adopting a model predictive control approach and considering the desired trajectory X^* and corresponding input U^*, the optimization problem for each iteration is given by

$$\begin{aligned} &\underset{U,X}{\text{minimize}} \quad J \\ &\text{subject to} \\ &\qquad \ddot{\theta}_1 = \frac{\tau_1}{J_1}, \\ &\qquad \ddot{\theta}_2 = \frac{\tau_2}{J_2}, \\ &\qquad \ddot{\theta}_b = \frac{T_2\cos(\theta_2-\theta_b) - T_1\cos(\theta_1-\theta_b)}{J_b + m\frac{c^2}{2}}, \\ &\qquad \ddot{x}_b = -\frac{\sin(\theta)T}{2m+m_b}, \\ &\qquad \ddot{z}_b = -g + \frac{\cos(\theta)T}{2m+m_b}, \end{aligned} \tag{31}$$

where $T = T_1 + T_2$. The results of the simulations are presented in section 8.

6. Control of the quadcopters bar system

This section covers the control design for the quadcopter bar system. The equations of motion of the system are defined in equations (26) and (28) present in section 4.2.

Cost function

In this example, the control objectives are system stabilization and trajectory optimization. Thus, it was considered appropriate to use a quadratic function for the cost function, where the deviation from the desired setpoints is measured. The cost function is given by

$$\begin{aligned} J = \sum_{i=1}^{H} &[(X(k+i) - X^*(k+i))^T Q (X(k+i) - X^*(k+i)) + \\ &+ (U(k+i) - U^*(k+i))^T R_Q (U(k+i) - U^*(k+i))] \end{aligned} \tag{32}$$

where Q and R_Q correspond, respectively, to the weight factors that are applied to the states and to the control inputs.

Optimization problem

Adopting a model predictive control approach and considering the desired trajectory X^* and corresponding input U^*, the optimization problem for each iteration is now defined

$$\begin{aligned} &\underset{U_1,U_2,X_1,X_2,X_b}{\text{minimize}} \quad J \\ &\text{subject to} \\ &\qquad \ddot{p}^I_b = -ge_3 + \frac{T_O}{m_{sys}}, \\ &\qquad I\dot{w}^{B_1} = -w^{B_1} \times Iw^{B_1} + \tau^{B_1}, \\ &\qquad I\dot{w}^{B_2} = -w^{B_2} \times Iw^{B_2} + \tau^{B_2}, \\ &\qquad I_{sys}\dot{w}^O = -w^O \times I_{sys}w^O + \tau^O. \end{aligned} \tag{33}$$

The results of the simulations are presented in section 8.

7. Drone replacement strategy

The benefit of addressing the problem of the drone autonomy is that the transport task performed through the cooperation of vehicles does not have to be interrupted if one of the drones has reached its maximum energy consumption and is unable to continue. Thus, if necessary, the replacement of drones can occur during the mission and the task can be carried out continuously until the end. The solution to this problem takes into account the replacement of UAVs and not batteries, since the latter situation would force the multi-drone system to stop.

Energy consumption model

In order to optimize the vehicle replacement process, it is necessary to efficiently manage the energy of each vehicle. For that purpose, this section addresses the problem of minimizing energy consumption of drones. Table 1 shows the values of the parameters used in the simulations present in this section.

	Symbol	Value
Mass of drone body [kg]	m_1,m_2	1
Mass of bar [kg]	m_{bar}	0.5
Drone battery energy [J/kg] [1]	E_0	5.4

Table 1: Adapted parameters for drone replacement problem.

The problem of minimizing the energy consumption of each vehicle introduces a state E_{C_i} for each

vehicle i ($i = 1, 2$), which represents the energy consumed by each drone per unit of time. Thus, the derivative of E_{C_i}, $\dot{E}_{C_i}$, represents the energy consumption rate of each drone per unit of time. The power corresponds to the rate of the work that is performed, whose formula is proportional to the force times the speed. Therefore, by analogy, $\dot{E}_{c_i}$ is given by

$$\dot{E}_{C_i} = K_i \left| v_i^T \dot{v}_i \right| + \left| w_i^T I_i \dot{w}_i \right|, \quad i = 1, 2, \tag{34}$$

where $K_i = m_i + m_{bar}\gamma$, ($i = 1, 2$) is a coefficient that describes the impact of the weight of the vehicle and the weight of the bar on the energy consumption rate of the drone. In this coefficient, a binary decision variable γ was adopted. This variable has two possible states: if $\gamma = 1$, the drone in question is carrying the bar and if $\gamma = 0$, the bar is not being transported. Based on the value of the parameters defined above, it is concluded that the weight of the bar adds a 50% energy expense to the energy consumption rate of each vehicle, since $K_i = 1.5$, when $\gamma = 1$.

Note that the energy available for each drone per unit of time, E_{D_i}, is given by

$$E_{D_i} = E_0 - E_{C_i}, \tag{35}$$

where E_0 corresponds to the battery energy for each drone.

Suboptimal solution to the optimal state transfer problem

Consider a drone (drone 1) that departs from the base station located at $(x, y) = (0, 0)$, carrying a bar. It is assumed that this vehicle does not have enough energy available to reach a predefined final position. Thus, the intervention of another vehicle is necessary. More precisely, drone 2 departs from the same station and meets his peer, at a given moment. From that moment, drone 2 will transport the bar, until the end of the predefined trajectory. In this context, it is also assumed that

- Each drone is able to transport the bar.
- For the sake of simplicity, it is considered that the bar is a mass point and that the battery energy value for each drone is $E_0 = 5.4\ J$ (previously defined in Table 1.
- Drone 2 will depart from the base at a moment when drone 1 has low battery (less than 30%), that is, in the time interval where $E_{D_1} =]0, 0.3E_0]$.
- In this scenario, charging stations are not considered.

Regarding the replacement of drone 1, a question arises: **What will be the optimum moment, t_1, when drone 2 should depart from the base in order to assist drone 1, with the objective of minimizing the energy consumption of both vehicles?** The purpose of this section is to find the answer to this question.

System under analysis

The system under analysis incorporates two continuous dynamic systems and, in addition to the control variables associated with each vehicle, an independent decision control variable: the switching time, t_1. In this problem, the system is divided as follows

- Subsystem 1, $\dot{x_1} = f_1(x_1, u_1)$, which is active in the interval $\left[t_0, \quad t_1\right]$, where $t_0 = 1$, in discrete time.
- Subsystem 2, $\dot{x_2} = f(x_2, u_2)$, which is active in the interval $\left[t_1 + 1, \quad t_f\right]$.

In Fig. 8, the problem under analysis is represented.

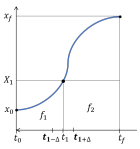

Figure 8: Explanation of the energy consumption optimization problem.

The trajectory of the system starts at a given initial state, x_0, and progresses to a final state, x_f. The state X_1 marks the transition between the first and the second set of dynamics. The problem then lies in deciding the optimal instant time, t_1, where the switch should be made. In order to solve this problem, an algorithm was proposed, that calculates t_1 through a search made by intervals, based on the minimum cost associated with each instant of time. For this purpose, an initial estimate is defined, $\hat{t_1}$, contained in the candidate values for t_1.

Optimization Problem

In this example, two different scenarios are considered for transporting the bar.

- **Case 1** - In this situation, it is considered that both vehicles are symmetrical. That is, they have the same mass and the same geometry.
- **Case 2** - In this case, drone 1 follows the description of the vehicles considered in case 1, while drone 2 presents a difference in geometry

which causes that, when transporting the bar, it consumes more battery than the first drone. The value considered for the mass of the bar is now $m_{bar} = 0.9\ kg$. Thus, when drone 2 transports the bar, there is an additional energy expense of 90% to its energy consumption rate, instead of the 50% expenditure considered in the previous case.

For both problems, there are three variants of the energy consumption model, depending on what time the system is operating.

– From $k = 1$ to $k = t_1$, the dynamics of drone 1 are active, with the following energy consumption model

$$\dot{E}_{C_1} = K_1 \left| v_1^T \dot{v}_1 \right| + \left| w_1^T I_1 \dot{w}_1 \right|, \tag{36}$$

where $K_1 = m_1 + m_{bar}$.

– From $k = t_1 + 1$ to $k = t_f$, the dynamics of drone 2 are active, and its corresponding energy model varies depending on the time interval in which dynamics 2 is acting. Its energy consumption model is given by

$$\dot{E}_{C_2} = K_2 \left| v_2^T \dot{v}_2 \right| + \left| w_2^T I_2 \dot{w}_2 \right|, \tag{37}$$

where

$$\begin{cases} K_2 = m_2, & k = t_1 + 1, \cdots, t_2 - 1. \\ K_2 = m_2 + m_{bar}, & k = t_2, \cdots, t_f. \end{cases}$$

System dynamics

For this example, the dynamics of each vehicle is active at different times. Note that the dynamics of the system is composed of the dynamics of each drone and also the respective model of energy consumption defined in (36) and (37). That is, from $k = 1$ to $k = t_1$, the following dynamics are active

$$\begin{aligned} & I\dot{w}^{B_1} = -w^{B_1} \times Iw^{B_1} + \tau^{B_1}, \\ & (m_1 + m_{bar})\ddot{p}_1 = -(m_1 + m_{bar})ge_3 + T_1 R^I_{B_1} e_3, \\ & \dot{E}_{C_1} = K_1 \left| v_1^T \dot{v}_1 \right| + \left| w_1^T I_1 \dot{w}_1 \right|, \end{aligned} \tag{38}$$

and from $k = t_1 + 1$ to $k = t_f$ the active dynamics is given by

$$\begin{aligned} & I\dot{w}^{B_2} = -w^{B_2} \times Iw^{B_2} + \tau^{B_2}, \\ & (m_2 + m_{bar}\gamma)\ddot{p}_2 = -(m_2 + m_{bar}\gamma)ge_3 + T_2 R^I_{B_2} e_3, \\ & \dot{E}_{C_2} = K_2 \left| v_2^T \dot{v}_2 \right| + \left| w_2^T I_2 \dot{w}_2 \right|. \end{aligned} \tag{39}$$

Cost function

In this example, the cost functions represent different control objectives, and are the following

- J_1 and J_2 are the costs associated with the movement of drone 1 and drone 2, respectively. J_1 is defined from the instants $k \in 1, \ldots, t_1$ and J_2 is computed from the instant immediately after the switching instant, t_1, until the final simulation instant, t_f.
- J_{opt_1} and J_{opt_2} are the costs associated with minimizing the energy consumption of each drone that express the objective of finding an optimal flight speed in order to maximize the distance traveled by each vehicle. That is, it expresses the objective of minimizing the energy consumption of each drone. J_{opt_1} is calculated in the same time interval as J_1 as J_2 and J_{opt_2} are calculated in the same period of time.

Since J_{opt_1} and J_{opt_2} have different control objectives than J_1 and J_2, it is considered appropriate to use the module in the definition of these cost functions, in order to minimize the energy consumption of each vehicle per unit of time. This is a usual choice for energy consumption minimization but other options could have could been made, taking into account convex functions of X_1, X_2, U_1 and U_2, as long as its definition was in line with the control objectives required by J_{opt_1} and J_{opt_2}. The cost functions considered in this problem are then given by

$$\begin{aligned} J_1 &= \sum_{i=1}^{H} [(X_1(k+i) - X_1^*(k+i))^T Q (X_1(k+i) - X_1^*(k+i)) + \\ &\quad + (U_1(k+i) - U_1^*(k+i))^T R_Q (U_1(k+i) - U_1^*(k+i))], \\ J_2 &= \sum_{i=1}^{H} [(X_2(k+i) - X_2^*(k+i))^T Q (X_2(k+i) - X_2^*(k+i)) + \\ &\quad + (U_2(k+i) - U_2^*(k+i))^T R_Q (U_2(k+i) - U_2^*(k+i))], \\ J_{opt_1} &= \sum_{i=1}^{H} [E_{C_1}(k+i) - \Gamma(\|v_1(k+i)\|^2], \\ J_{opt_2} &= \sum_{i=1}^{H} [E_{C_2}(k+i) - \Gamma(\|v_2(k+i)\|^2)]. \end{aligned} \tag{40}$$

where Γ is a coefficient that when $\Gamma > 1$, attaches more importance to minimizing the energy consumption of the respective drone and when $\Gamma < 1$, it gives more importance to optimizing the velocity at which the vehicle moves. Additionally, Q and R_Q correspond, respectively, to the weight factors that are applied to the states and to the control inputs of both vehicles.

Optimization problem

The optimization problem for each iteration is now defined

$$\begin{aligned} & \underset{U_1, U_2, X_1, X_2, t_1}{\text{minimize}} \quad J_{1_{k\in 1,\ldots,t_1}} + J_{opt_{1_{k\in 1,\ldots,t_1}}} + J_{2_{k\in t_1+1,\ldots,t_f}} + J_{opt_{2_{k\in t_1+1,\ldots,t_f}}} \\ & \text{subject to} \\ & \quad for\ \ k = 1, \cdots, t_1 \\ & \quad\quad I\dot{w}^{B_1} = -w^{B_1} \times Iw^{B_1} + \tau^{B_1}, \\ & \quad\quad (m_1 + m_{bar})\ddot{p}_1 = -(m_1 + m_{bar})ge_3 + TR^I_{B_1} e_3, \\ & \quad\quad 0 < E_1 < E_0, \\ & \quad\quad \dot{E}_{C_1} = K_1 \left| v_1^T \dot{v}_1 \right| + \left| w_1^T I_1 \dot{w}_1 \right|. \\ & \quad for\ \ k = t_1 + 1, \cdots t_f \\ & \quad\quad I\dot{w}^{B_2} = -w^{B_2} \times Iw^{B_2} + \tau^{B_2}, \\ & \quad\quad (m_2 + m_{bar}\gamma)\ddot{p}_2 = -(m_2 + m_{bar}\gamma)ge_3 + TR^I_{B_2} e_3, \\ & \quad\quad 0 < E_2 < E_0, \\ & \quad\quad \dot{E}_{C_2} = K_2 \left| v_2^T \dot{v}_2 \right| + \left| w_2^T I_2 \dot{w}_2 \right|. \\ & \quad p_1(t_2) = p_2(t_2). \end{aligned} \tag{41}$$

where

$$\begin{cases} \gamma = 0, & k = t_1, \cdots, t_2 - 1. \\ \gamma = 1, & k = t_2, \cdots, t_f. \end{cases}$$

The results of the simulations are presented in section 8.

8. Simulations Results

This section shows some of the simulation tests that validate the models previously described.

8.1. Bi-rotor bar model

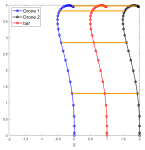

Figure 9: System trajectory for $H = 10$, $T_s = 0.3$.

8.2. Quadcopters transporting a bar

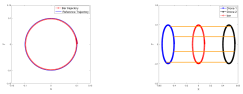

(a) Bar trajectory (b) System trajectory

Figure 10: System trajectory for $H = 12$, $T_s = 0.2$ and $x(0) = \begin{bmatrix} 0.1\cos(0.01\pi) & 0.1\sin(0.01\pi & 0 \end{bmatrix}^T$.

8.3. Drone replacement strategy

The candidate values of t_1 are chosen in a time interval when the energy available of drone 1 per unit of time, E_{D_1}, is less than or equal to 30% of its initial energy, E_0. Fig. 11 shows the candidate values for t_1 that are present in this interval (Δt), defined from $t_1 = 13$ to $t_1 = 16$, in discrete time. After $k = 16$, the instants of time are not considered candidate values of t_1 since the transport of the bar by drone 2 happens at $t_2 = t_1 + 3$. Thus, it is necessary to wait 3 samples after the instant t_1 for the transport of the bar to occur and 1 sample to observe its effects, in discrete time.

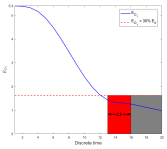

Figure 11: Choice of candidate values for t_1 present in Δt.

In the simulation shown in Fig. 12, the evolution of the total cost value, J_{total}, is represented for each candidate for t_1, ($t_1 = 13, 14, 15, 16$) in both cases. The optimal switching time found for both cases is $t_1 = 1.6$ seconds, since J_{total} is minimal for that instant of time.

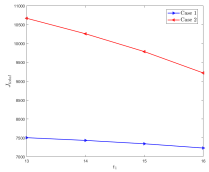

Figure 12: Total cost of both situations for $H = 26$ and $T_s = 0.1$.

Fig. 13 shows the energy consumption of the two vehicles for both scenarios. These two situations have four time periods in common, represented in the figure by gray circles, dictated by the behavior of drones.

1. Drone 1 starts the course while drone 2 waits to intervene.
2. The beginning of this period marks the transition from dynamics 1 to the dynamics of the second vehicle. After this switch, which occurs at the optimum time t_1, only drone 2 is in motion.
   (a) During this time, drone 2 is in motion, without carrying the bar.
   (b) The initial moment of this interval, $t_2 = t_1 + 0.3$ seconds, marks the meeting of the drones. From this moment on, the second vehicle will carry the bar.

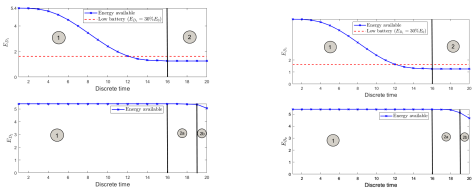

(a) Case 1 (b) Case 2

Figure 13: Vehicle energy consumption for both cases.

9. Conclusions

The objective of this work was to develop a controller in order to solve the problem of transporting large objects by a multi-drone system. This purpose was achieved through a strategy based on nonlinear predictive control algorithms. Additionally, the problem of performing missions with a duration that goes beyond the autonomy of a single drone in a multi-drone system was considered. The solution to this problem took into account the aforementioned non-linear MPC technique and a pseudo-algorithm of searching for the optimum instant of the departure of a second vehicle from the base so that the replacement of the vehicle occurs. At

the beginning of this study, the bi-rotor model was studied, whose knowledge was then applied to the analysis of a more complex system, composed of two bi-rotors that carry a bar. Subsequently, the quadcopter model was defined and this knowledge was applied to the study of a system composed of two drones that cooperate in order to transport a bar. For this system, it was considered a different configuration where the bar is connected to each drone through spherical joints, which allows the total mobility of both vehicles. In the following two chapters, the control strategies for the bi-rotor bar system and the quadcopter bar system were analyzed, respectively. In both cases, simulations were carried out in order to analyze the robustness of the controller through different maneuvers performed by the system. Finally, the last section of this work was dedicated to the problem of vehicle replacement. In this context, it was assumed that each vehicle was able to transport the bar individually. The problem was formulated in the following way: It was considered that a drone would depart from a given position in order to transport the bar to a defined final position. However, this vehicle did not have enough energy to complete the predefined trajectory. Thus, the need arose to introduce another UAV so that the second drone could depart from the base and meet his peer, in order to finish the rest of the trajectory, carrying the bar.

In conclusion, predictive control is a powerful tool due to its ability to allow the incorporation of restrictions into optimization problems. It is possible to solve problems of increasing complexity such as the transport problem carried out through the cooperation of two quadcopters, presented in this work. However, a compromise between the complexity of the problem to be addressed and the added computational burden of the problem must be taken into account. There are several research paths that can be followed, based on this work. On the one hand, the problem of transporting large objects by a multi-drone system can be explored through the proposal of a decentralized control approach. This would be an efficient solution to allow more drones to be included in the system, without compromising its performance. On the other hand, a more sophisticated approach to the problem of vehicle replacement could be considered. For example, a distributed strategy could be implemented so that drones could communicate and possibly provide a decentralized and scalable solution, robust to partial system failures.

References

[1] J. Zhang, J. Campbell, D. Sweeney and A. Hupman, "Energy Consumption Models for Delivery Drones: A Comparison and Assessment", *Project: Drone Delivery*, University of Missouri-St. Louis, May 2020.

[2] T. Kusznir and J. Smoczek, "Sliding Mode-Based Control of a UAV Quadrotor for Suppressing the Cable-Suspended Payload Vibration", *Journal of Control Science and Engineering*, vol.2020, 2020.

[3] European Comission, "Digital Transformation Monitor - Drones in Agriculture", January 2018.

[4] P. R. Grammatikis, P. G. Sarigiannidis, T. Lagkas, Thomas and I. Moscholios, "A Compilation of UAV Applications for Precision Agriculture", *Computer Networks*, vol.172, pp. 107-148, February 2020.

[5] R. Bonatti, W. Wang, C. Ho, A. Ahuja, M. Gschwindt, E. Camci, E. Kayacan, S.Choudhury and S. Scherer, "Autonomous aerial cinematography in unstructured environments with learned artistic decision-making", *Journal of Field Robotics*, vol.37, January 2020.

[6] M. Erdelj, O. Saif, E. Natalizio and I. Fantoni, "UAVs that Fly Forever: Uninterrupted Structural Inspection through Automatic UAV Replacement", *Ad Hoc Networks*, vol. 94, December 2017.

[7] Y. Wang, F. Xu and V. Puig, "Nonlinear Model Predictive Control with Constraint Satisfactions for a Quadcopter", *Journal of Physics: Conference Series*, vol.783, 2016.

[8] A. Torres-González, J. Capitán, R. Cunha, A. Ollero and I. Mademlis, "A Multidrone Approach for Autonomous Cinematography Planning", *Advances in Intelligent Systems and Computing*, pp.337-349, 2018.

[9] Z. Wang, S. Singh, M. Pavone and M. Schwager, "Cooperative Object Transport in 3D with Multiple Quadrotors Using No Peer Communication", *International Conference on Robotics and Automation*, pp. 1064-1071, 2018.

[10] Z. Wang, S. Singh, M. Pavone and M. Schwager, "Cooperative Object Transport in 3D with Multiple Quadrotors Using No Peer Communication", *2018 IEEE International Conference on Robotics and Automation (ICRA)*, pp. 1064-1071, 2018.

[11] R. Praveen Jain, "Transportation of cable suspended load using unmanned aerial vehicles: A real-time model predictive control approach", *Msc Thesis*, Delft University of Technology, 2015.